Electronic Supplementary Information

Fluorescein hydrazone based supramolecular architectures, molecular recognition, sequential logic operation and cell imaging

Kamini Tripathi, Abhishek Rai, Amarish Kumar yadav+, Saripella Srikrishna+ Niraj Kumari*and Lallan Mishra*

Department of Chemistry, Institute of Science, Banaras Hindu University, Varanasi, India.

+ Department of Biochemistry, Institute of Science, Banaras Hindu University, Varanasi, India

*E mail:nirajchem@gmail.com, lmishrabhu@yahoo.co.in; Fax: +91-542-2368127.

Contents

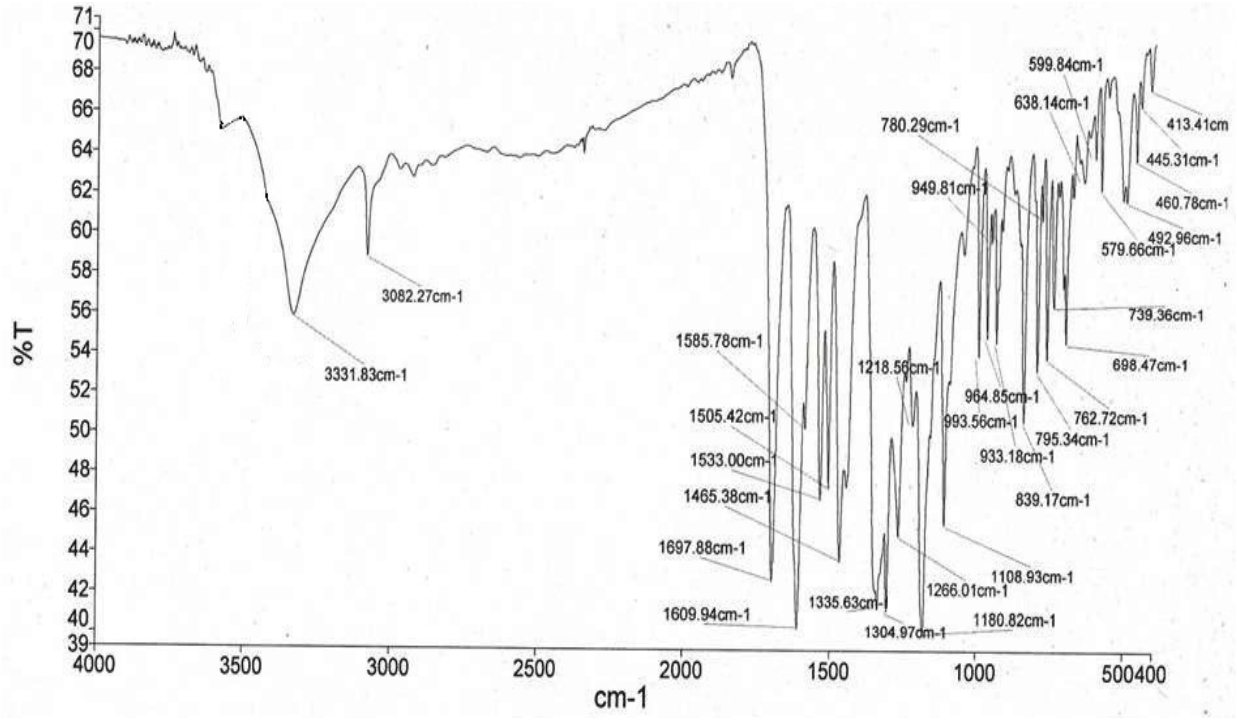

Figure S1. IR spectrum of **FDNS**

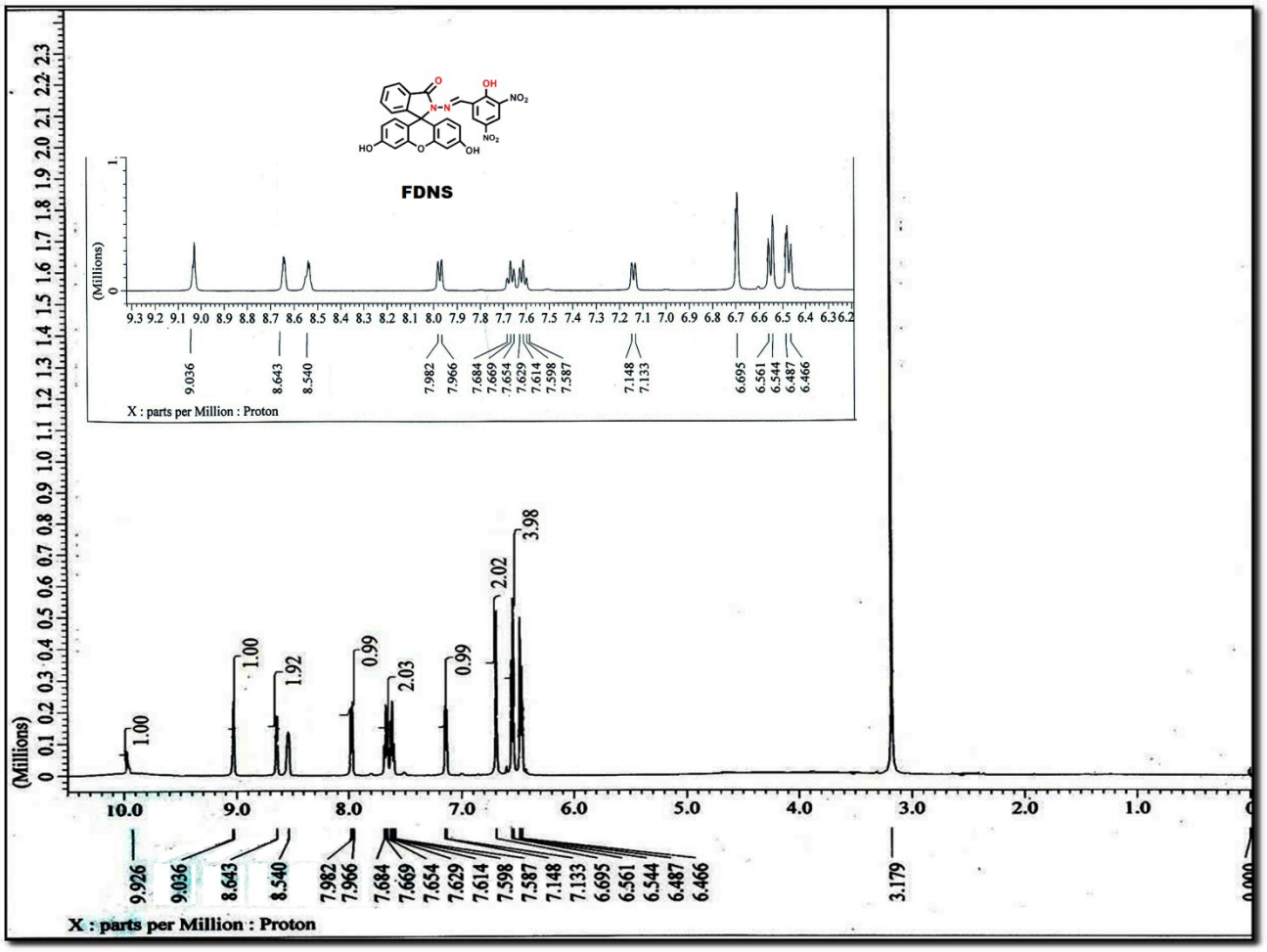

Figure S2. [1]H NMR spectrum of **FDNS** in DMSO,d6 at room temperature

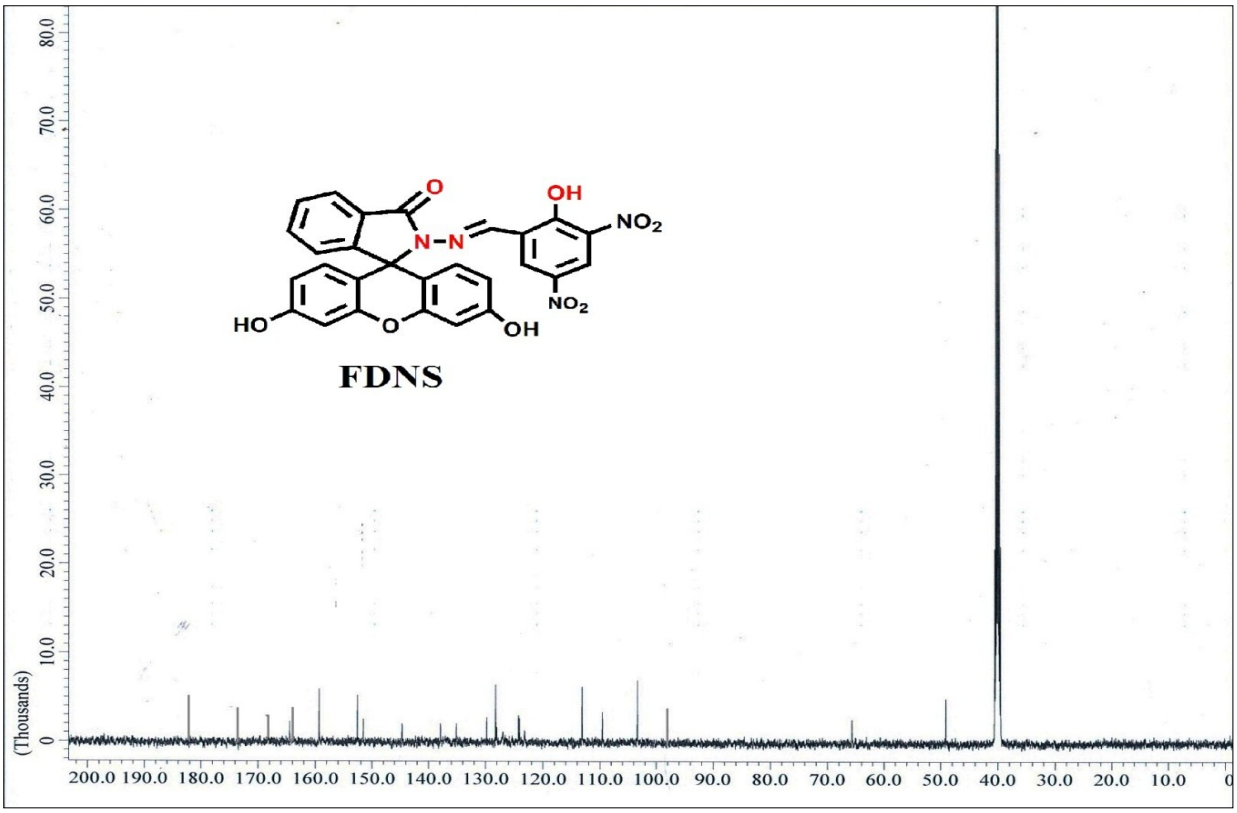

Figure S3. ^{13}C NMR spectrum of **FDNS** in DMSO,d6 at room temperature

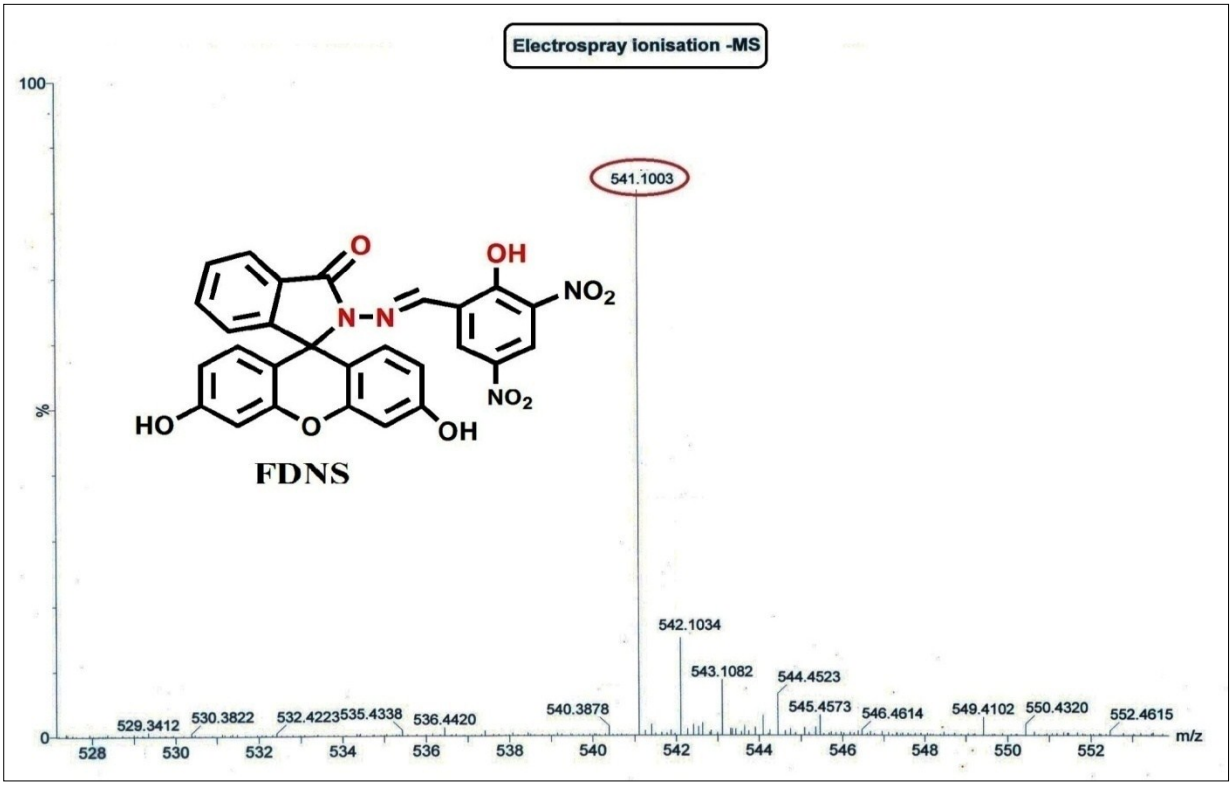

Figure S4. ESI- Mass spectrum of **FDNS**

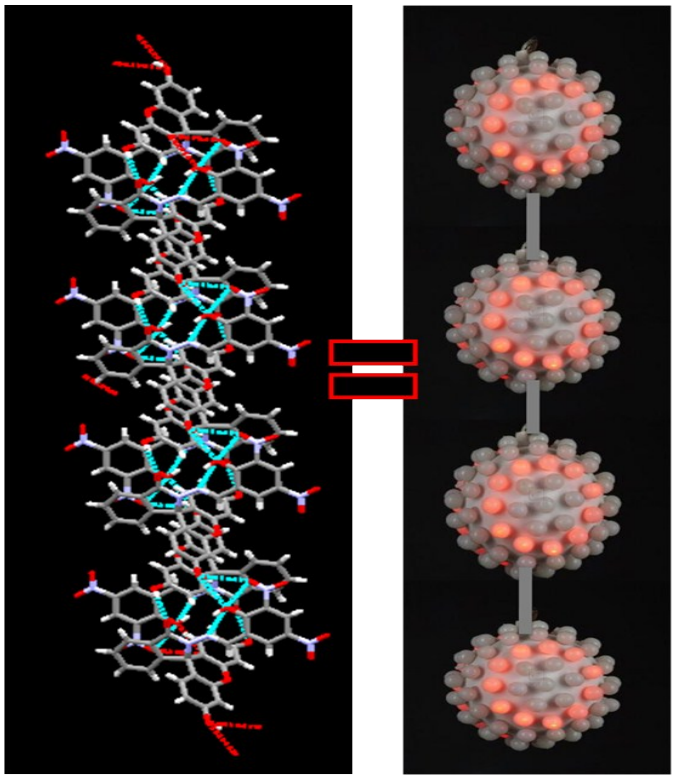

Figure S5. The packing structure of **FDNS** along 'a' axis as series of incandescent body connected via a single wire.*

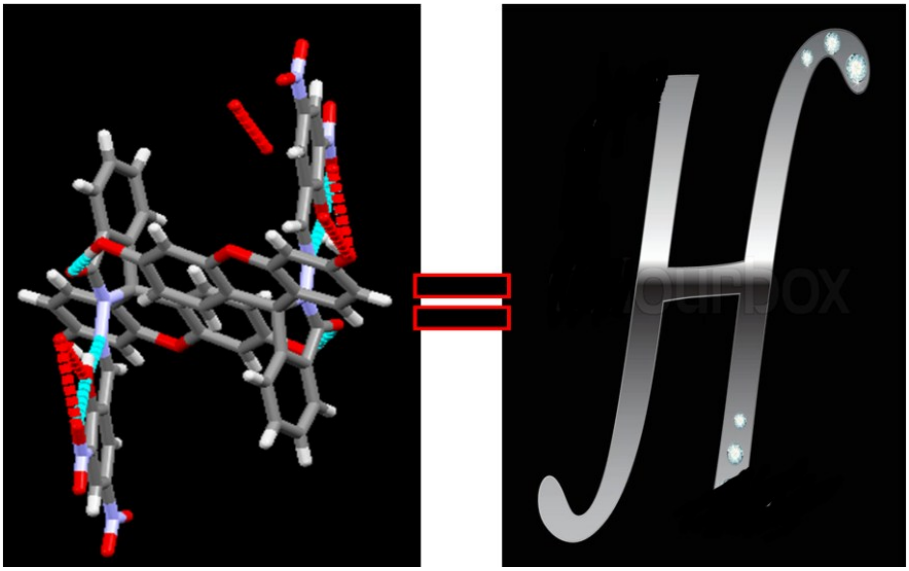

Figure S6. The packing structure of **FDNS** along 'c' axis as H-shaped structure.

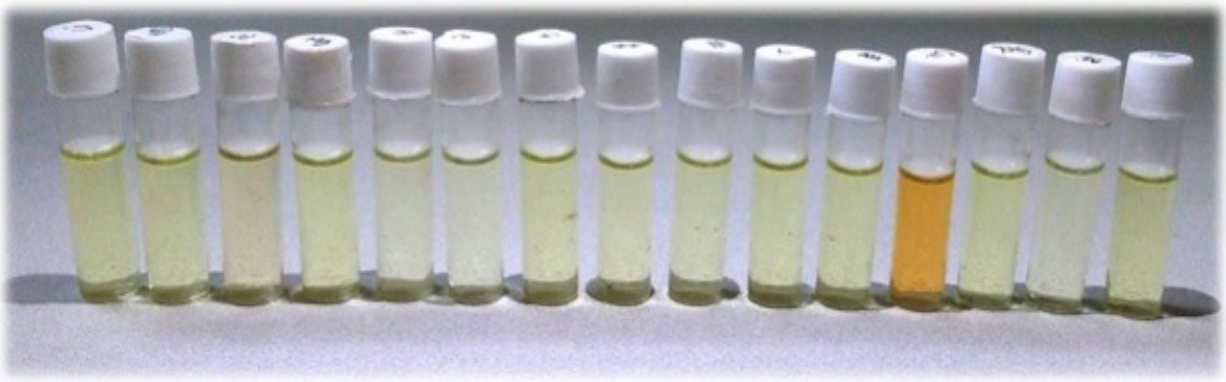

Figure S7. Colorimetric response of **FDNS** in a MeOH:aqueous (2 : 8 v/v) HEPES buffer (1mM, pH 7.4) in the presence of various metal ions (10 eq.) solution. From left to right: FDNS (10 μM), and FDNS with Li^{+},Hg^{2+},Ca^{2+} ,Cd^{2+}, Fe^{3+}, Na^{+}, Al^{3+}, Zn^{2+} ,Pb^{2+},Mg^{2+}, Cu^{2+} ,Co^{2+}, Ni^{2+}, and Ag^{+} ions

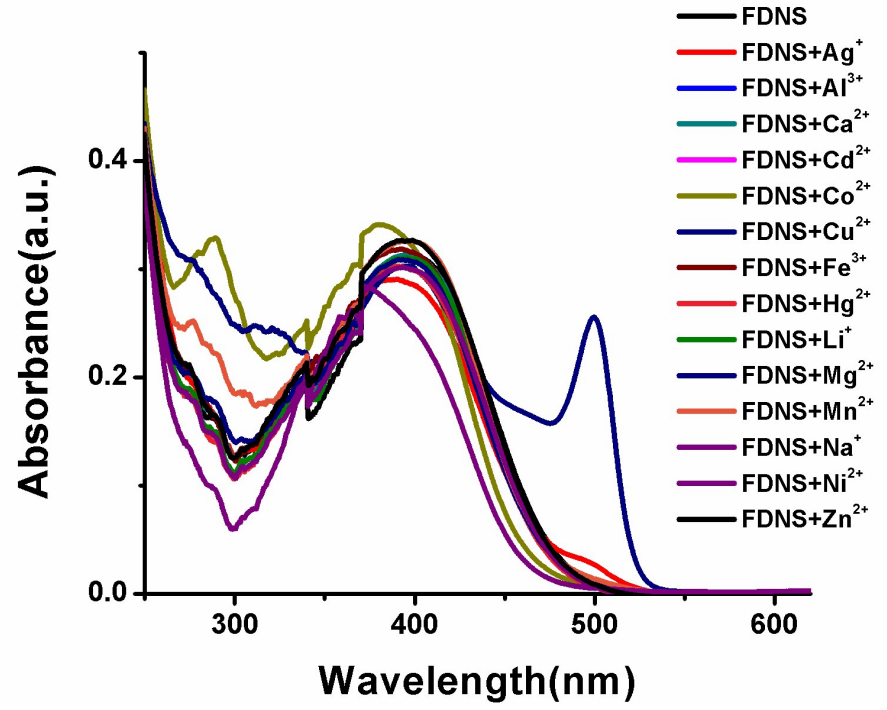

Figure S8. Changes of the absorption spectra of **FDNS** (10 μM) observed on addition of metal ions (Nitrate salts of Li^{+},Hg^{2+},Ca^{2+} ,Cd^{2+}, Fe^{3+}, Na^{+}, Al^{3+}, Zn^{2+} ,Pb^{2+},Mg^{2+}, Cu^{2+} ,Co^{2+}, Ni^{2+}, and Ag^{+} ions) (10 equiv) in a MeOH:aqueous (2 : 8 v/v) HEPES buffer (1mM, pH 7.4)

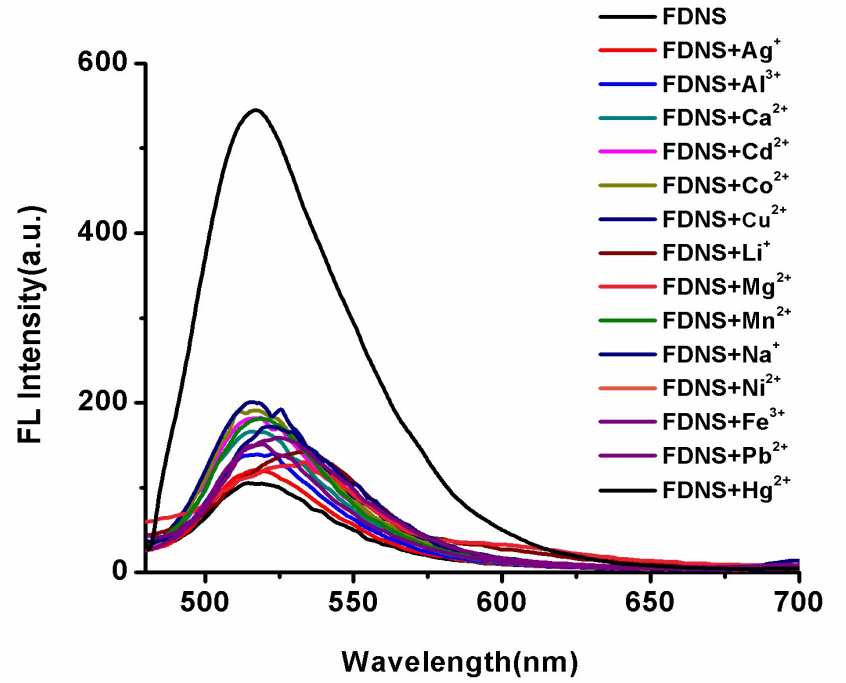

Figure S9. The flourescence spectra of **FDNS** (10 μM) observed on addition of metal ions (Nitrate salts of Li^{+},Hg^{2+},Ca^{2+} ,Cd^{2+}, Fe^{3+}, Na^{+}, Al^{3+}, Zn^{2+} ,Pb^{2+},Mg^{2+}, Cu^{2+} ,Co^{2+}, Ni^{2+}, and Ag^{+} ions) (10 equiv) in a MeOH:aqueous (2 : 8 v/v) HEPES buffer (1mM, pH 7.4)

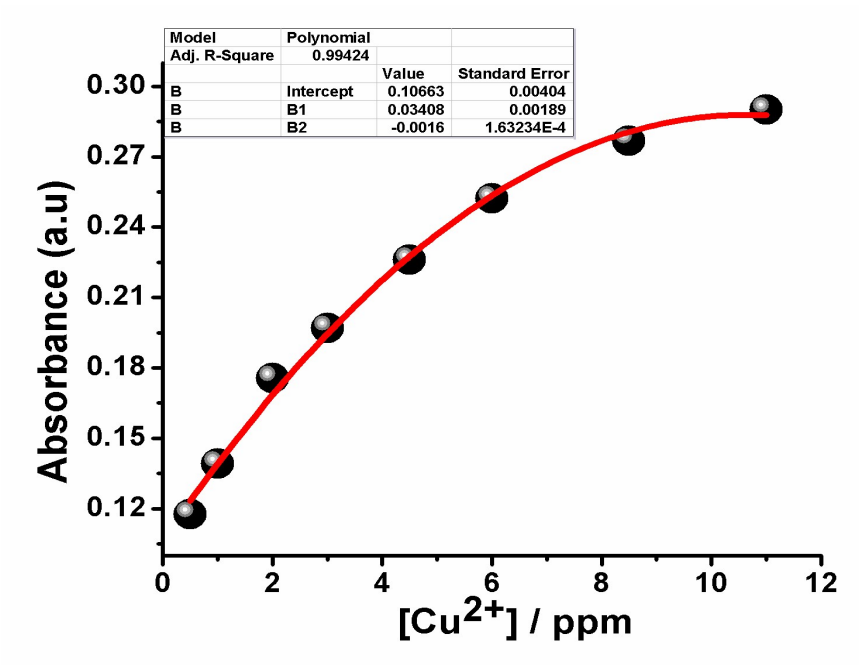

Figure S10. Graph of fluorescence intensity of **FDNS** as a function of concentrations of Cu^{2+} at ppm level in H_2O (R^2 =0.99).

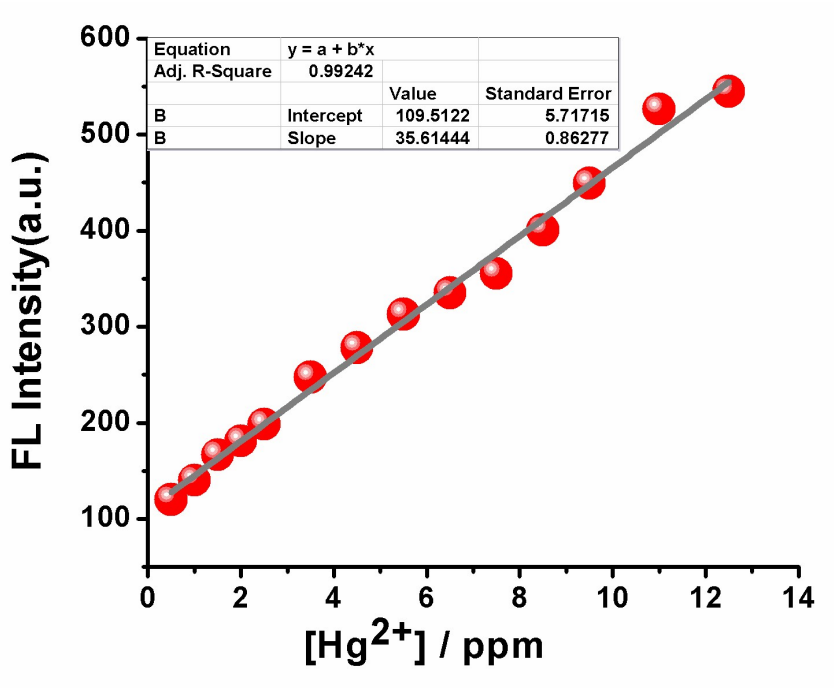

Figure S11. Graph of fluorescence intensity of **FDNS** as a function of concentrations of Hg^{2+} at ppm level in H_2O (R^2 =0.99).

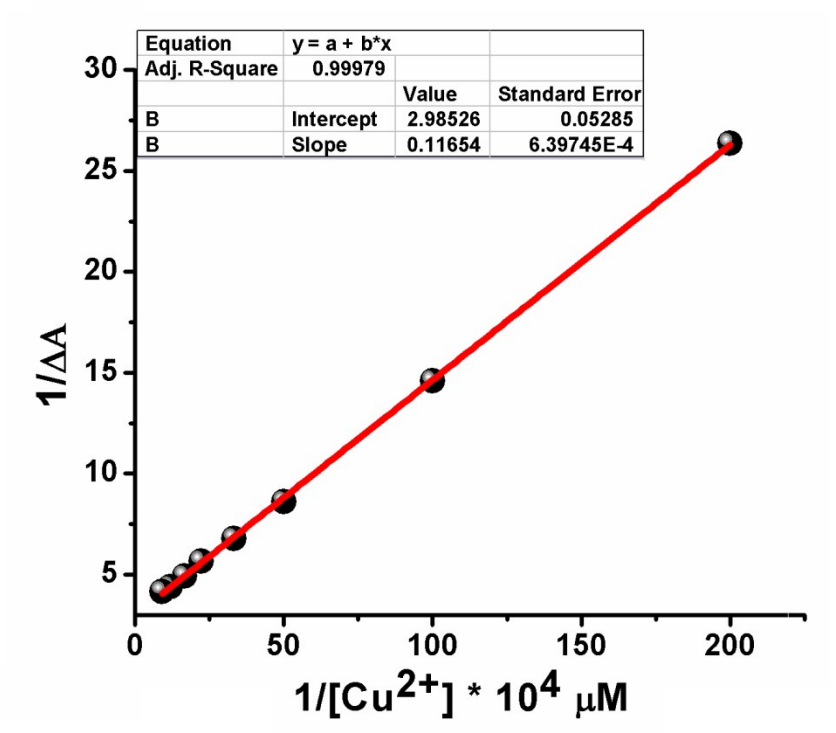

Figure S12. Benesi−Hildebrand (B−H) plot of **FDNS** –Cu^{2+}.

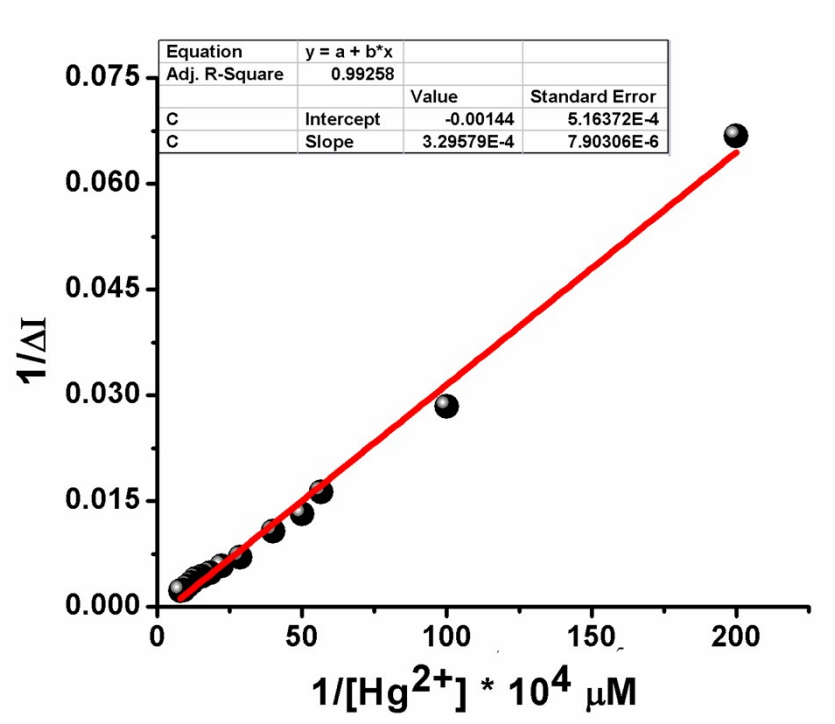

Figure S13. Benesi−Hildebrand (B−H) plot of **F**–Hg^{2+}

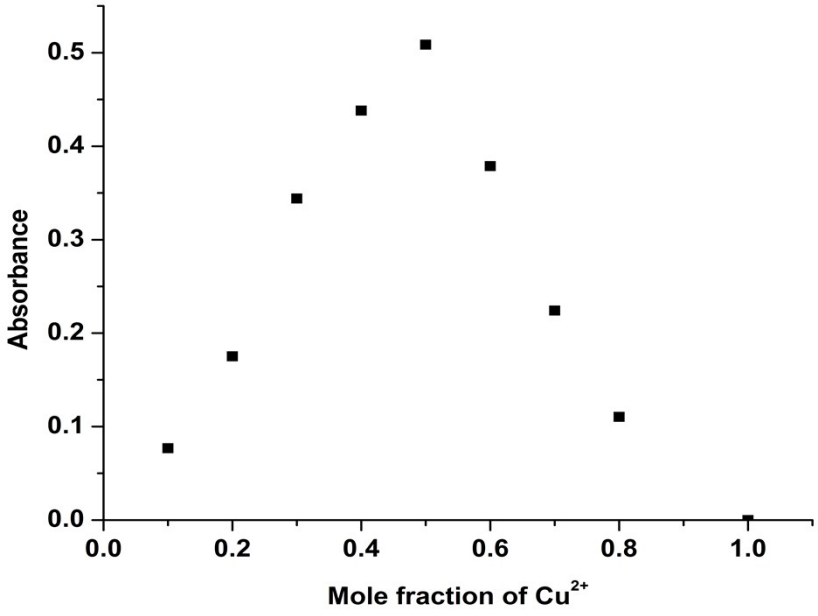

Figure S14. Job's plot of **FDNS** –Cu^{2+}adduct showing 1:1 binding ratio.

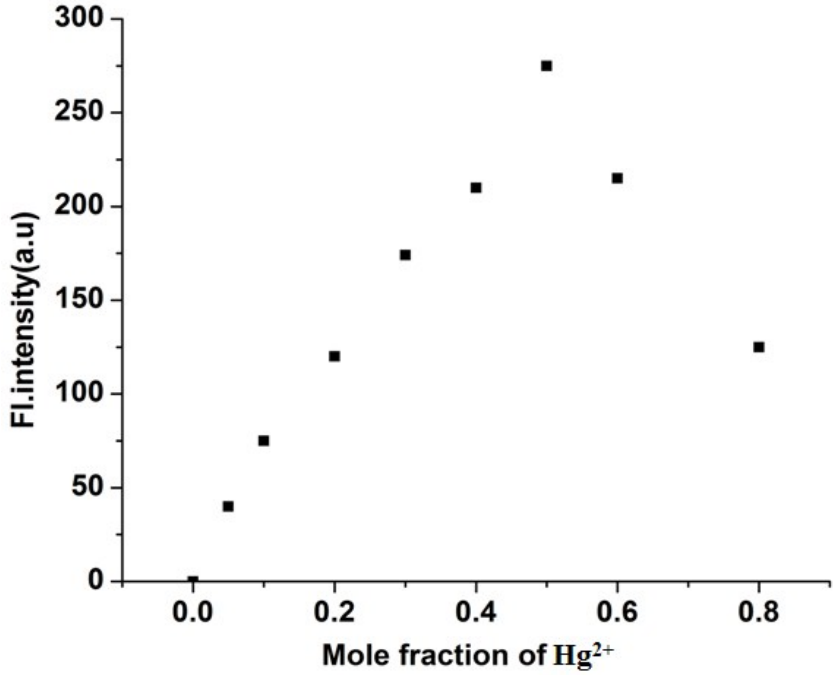

Figure S15. Job's plot of **FDNS**–Hg^{2+} adduct showing 1:1 binding ratio.

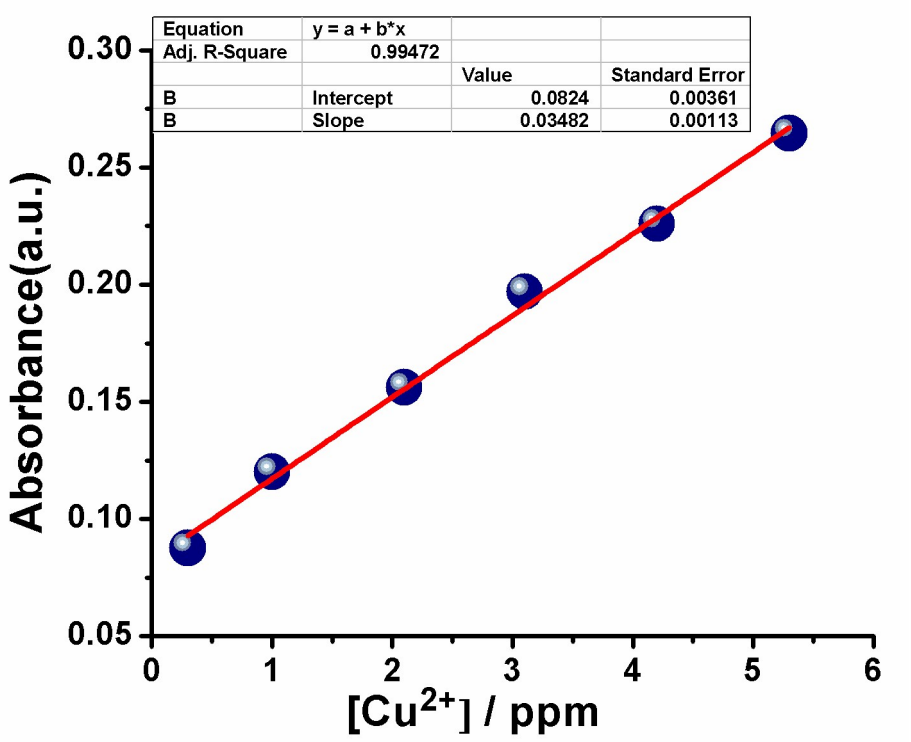

Figure S16. Calibration curve for determination of detection limit of **FDNS** for $Cu^{2+}$by using absorption titration data**.**

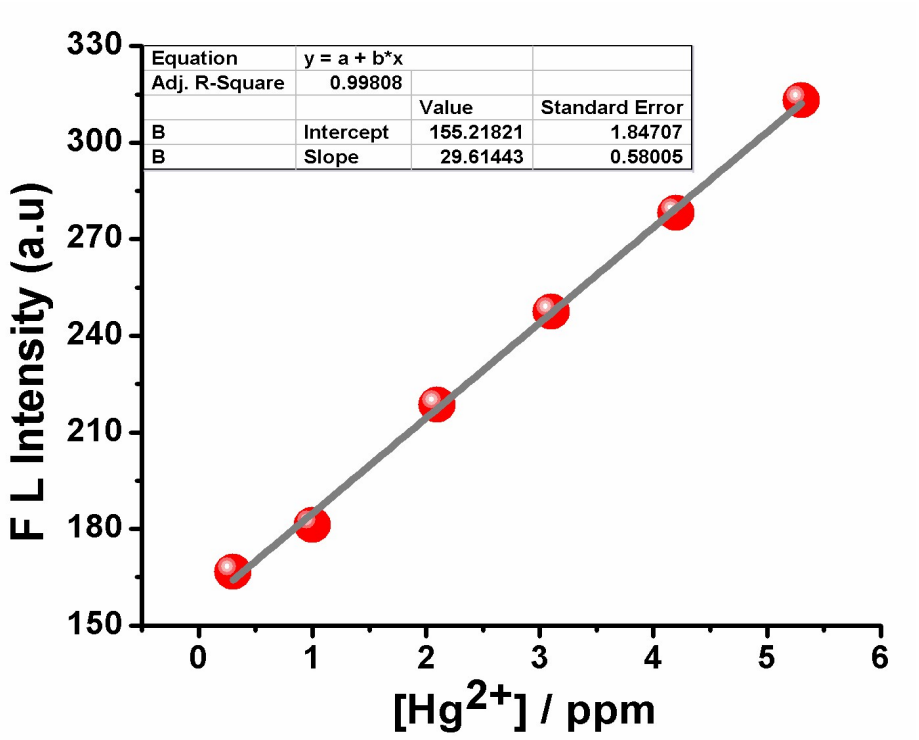

Figure S17: Calibration curve for determination of detection limit of **FDNS** for Hg^{2+} by using fluorescence titration data.

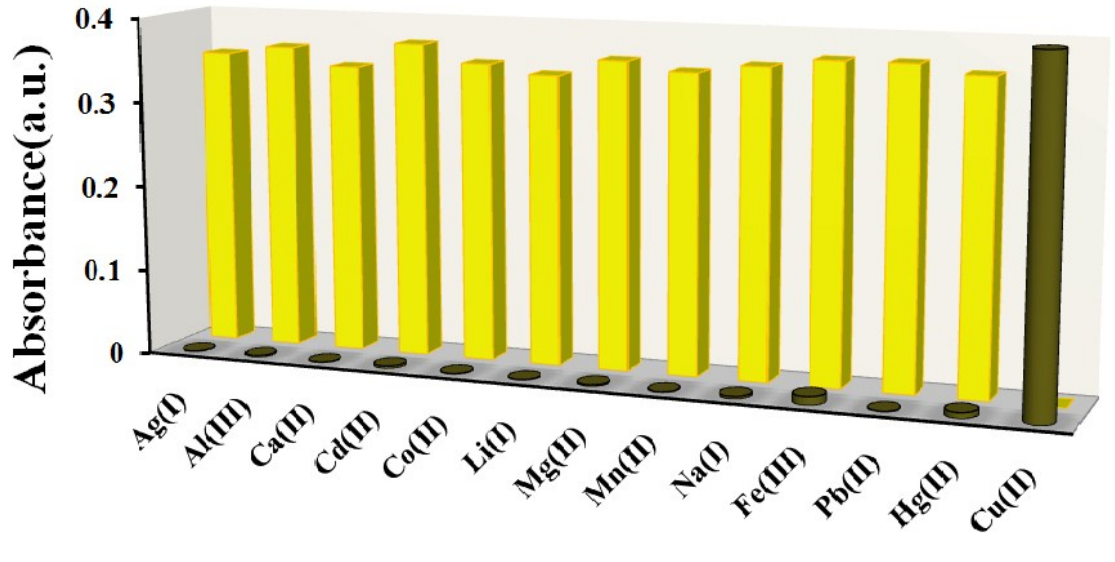

Figure S18. Bar graph representation of absorption spectrum for competition study **[olive green bars]** = **FDNS** in the presence of various cations, **[yellow bars]=FDNS**–Cu^{2+}, followed by various competing cations.

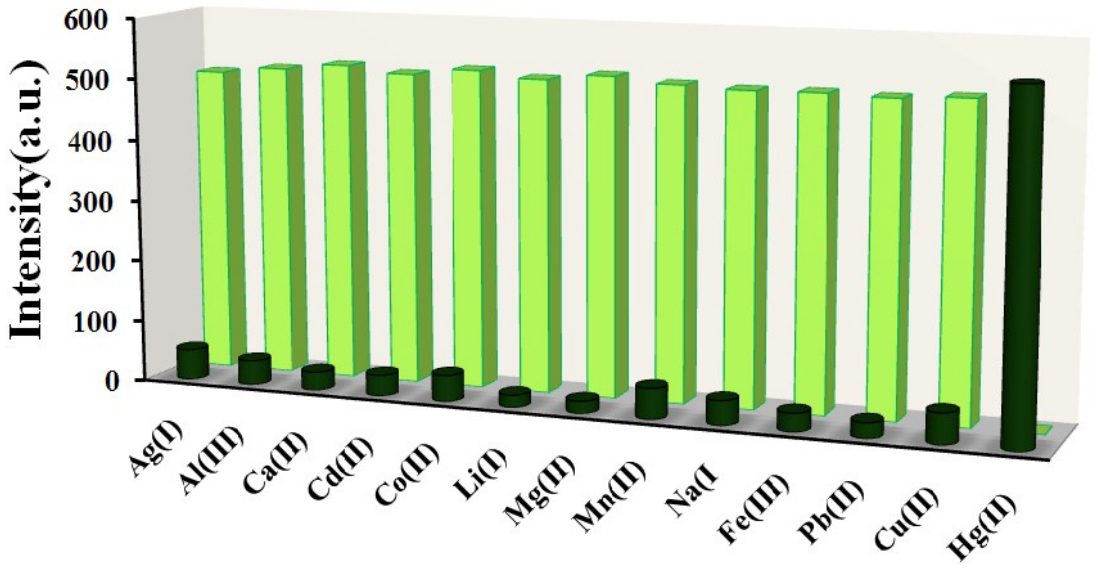

Figure S19. Bar graph representation of emission spectrum for competition study **[green bars]** = **FDNS** in the presence of various cations, **[light green bars]=FDNS**–Hg^{2+}, followed by various competing cations.

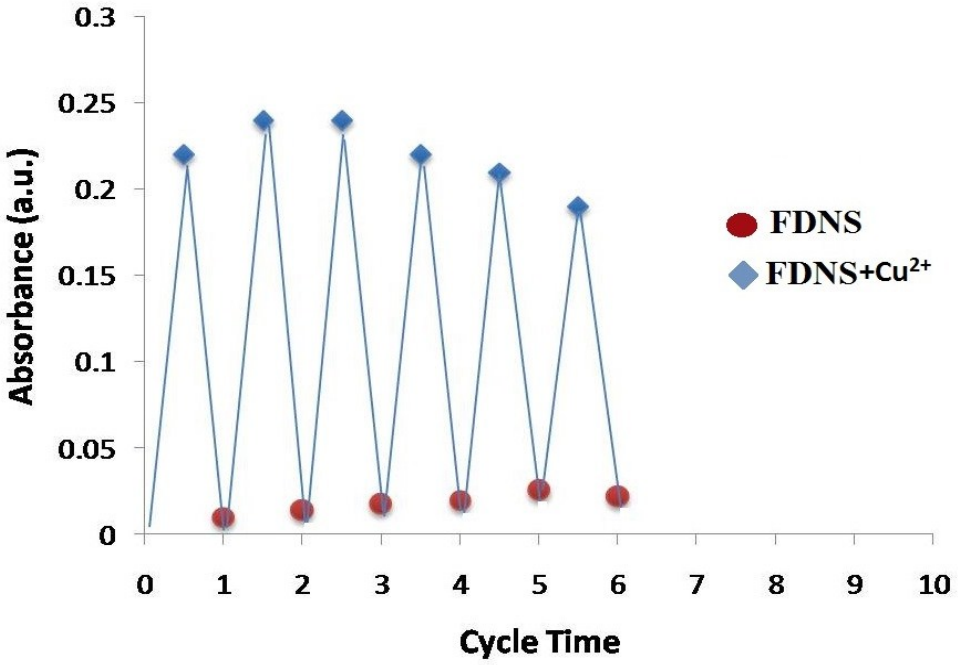

Figure S20 Reversibility cycle of **FDNS** evaluated by the alternative additions of Cu^{2+} and EDTA.

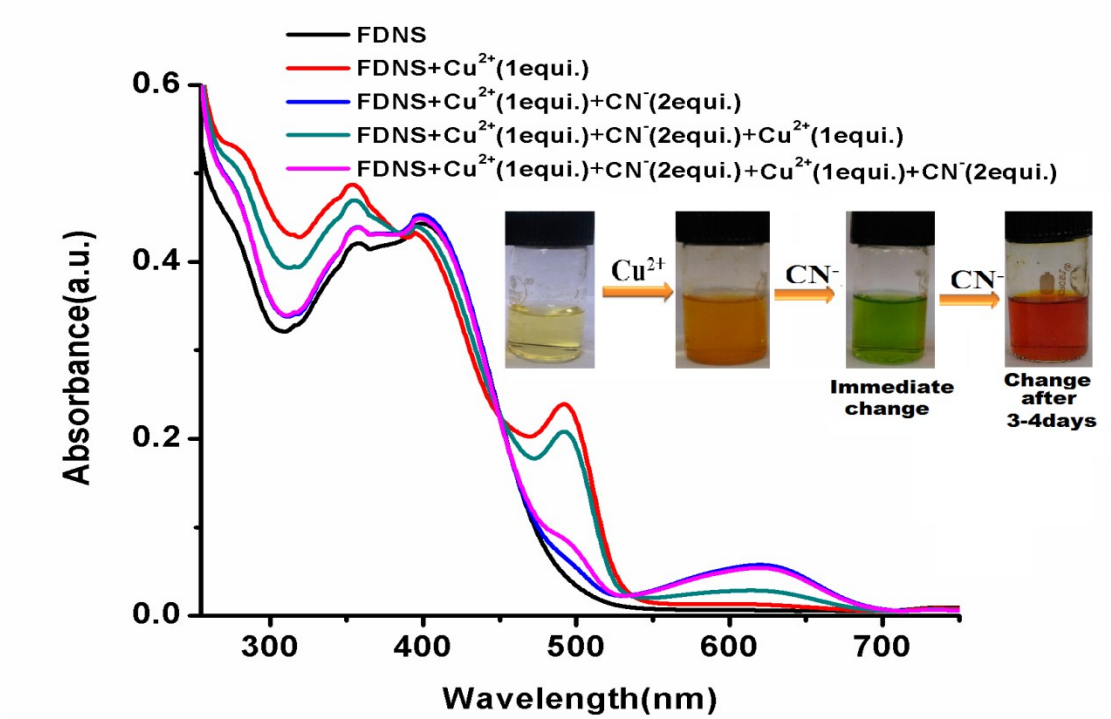

Figure S21. Repeatability of **FDNS** evaluated by the alternative additions of Cu^{2+} and CN^- (CN^- is 2equiv. to Cu^{2+}) alternately to the FDNS solution. Inset: Visual change in the color of FDNS solution in the presence of Cu^{2+} and CN^- under normal light.

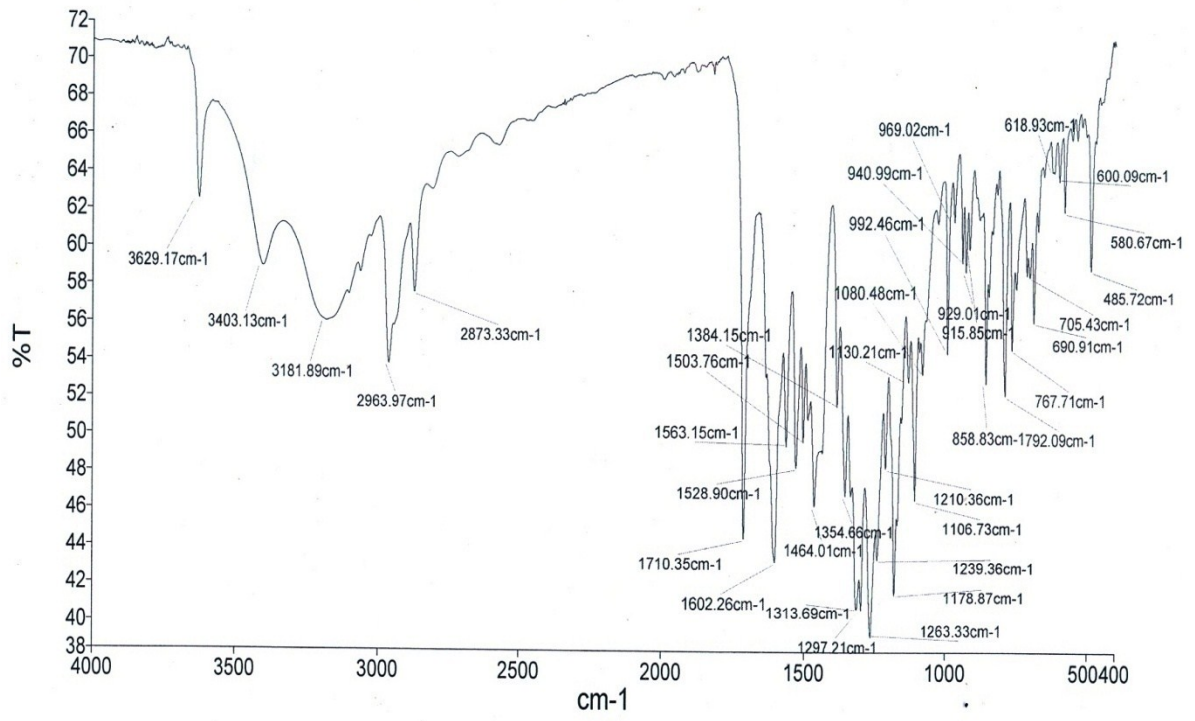

Figure S22. IR spectrum of **FKCN.**

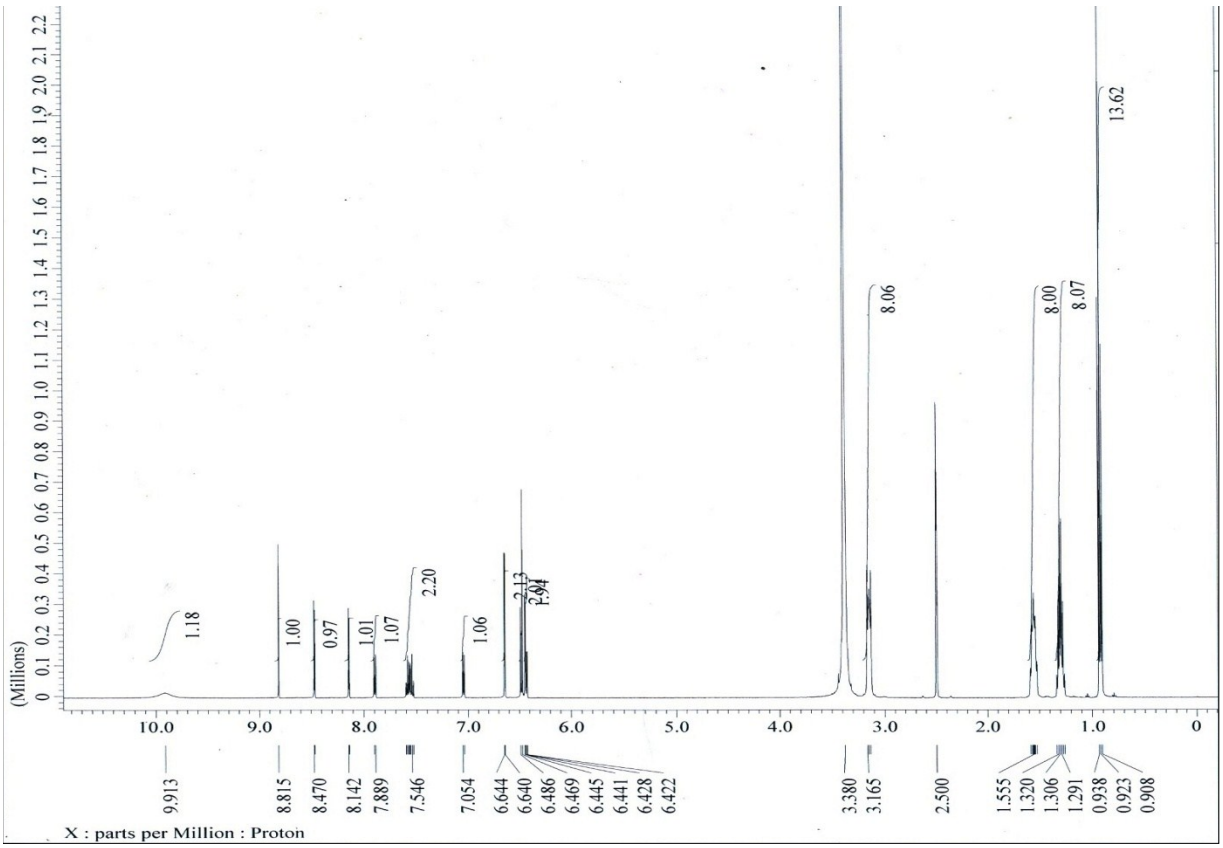

Figure S23. [1]H NMR spectrum of **FKCN** in DMSO,d6 at room temperature

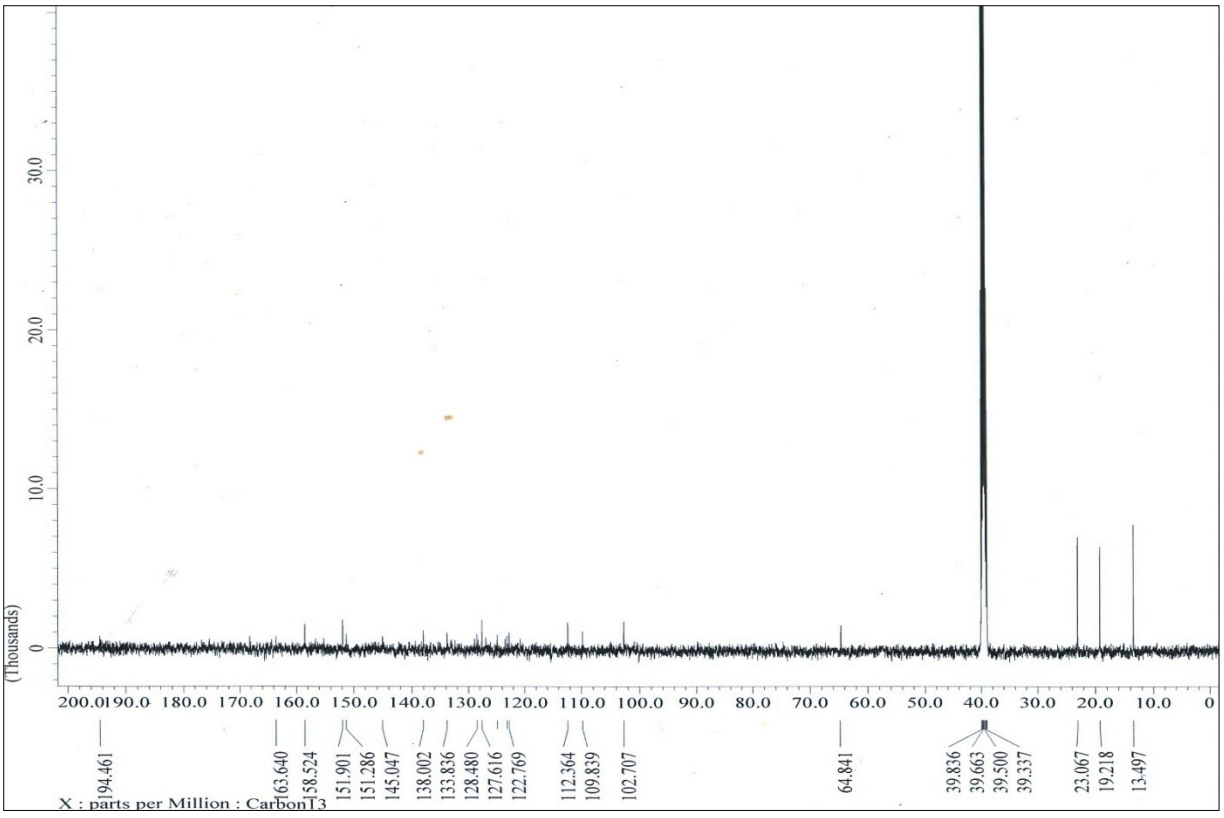

Figure S24. [13]C NMR spectrum of **FKCN** in DMSO,d6 at room temperature.

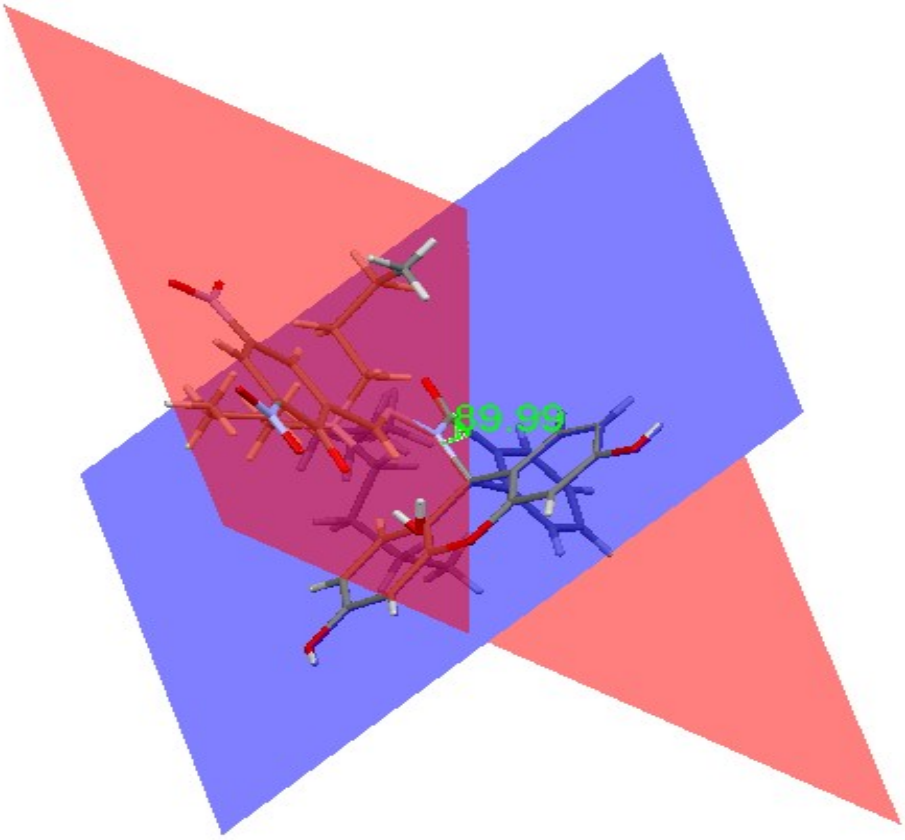

Figure S25. Molecular structure of paddle-wheel type model of **FKCN** where planes are passing through the center and dihedral between them is 89.99°.

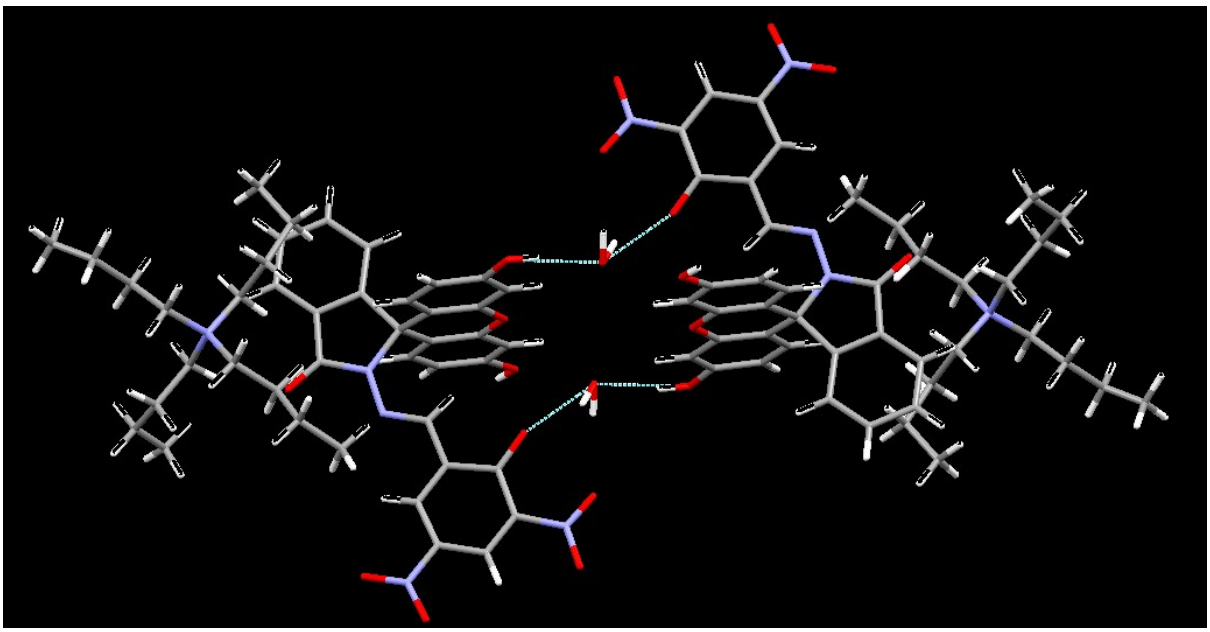

Figure S26. The packing structure of **FKCN** along 'c' axis shows cavity like structure.

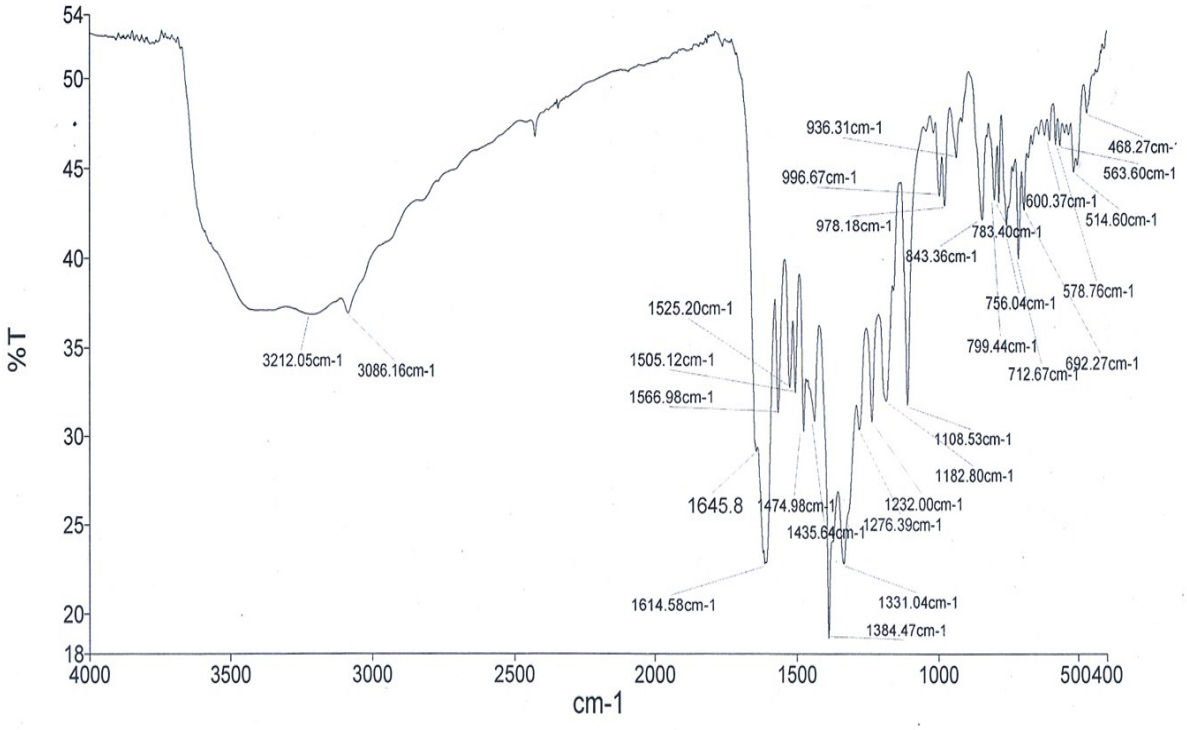

Figure S27. IR spectrum of **FDNS**–Cu^{2+}

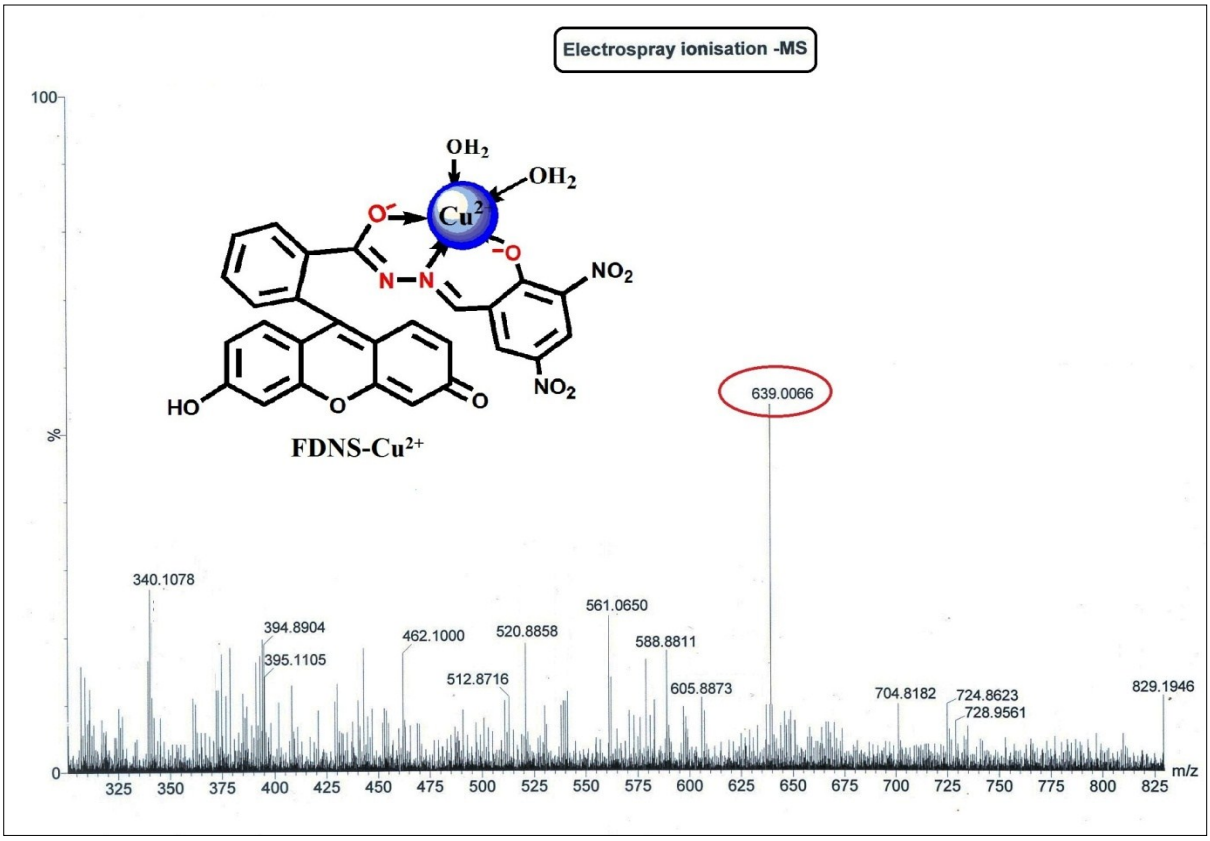

Figure S28. ESI- Mass spectrum of **FDNS**–Cu^{2+}

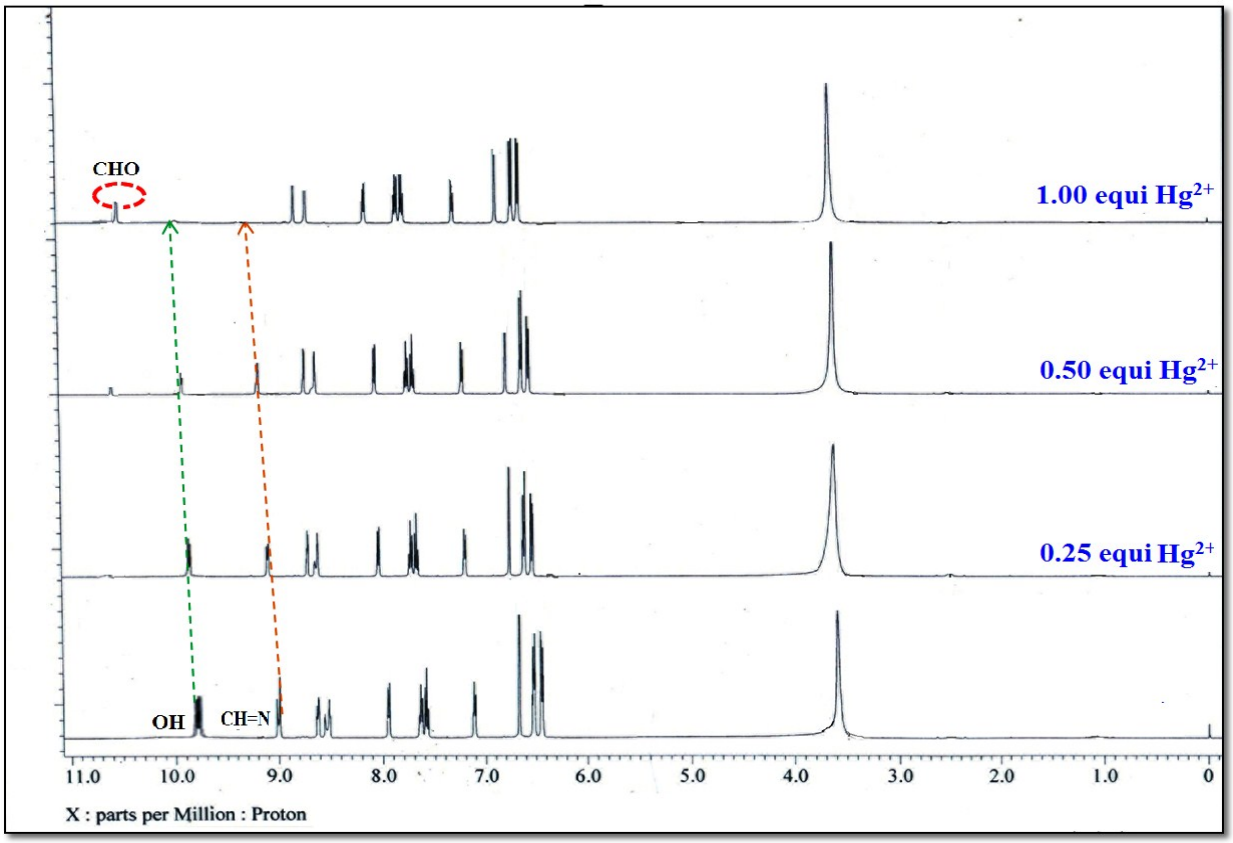

Figure S29. ^{1}H NMR titration **FHY**–Hg^{2+}

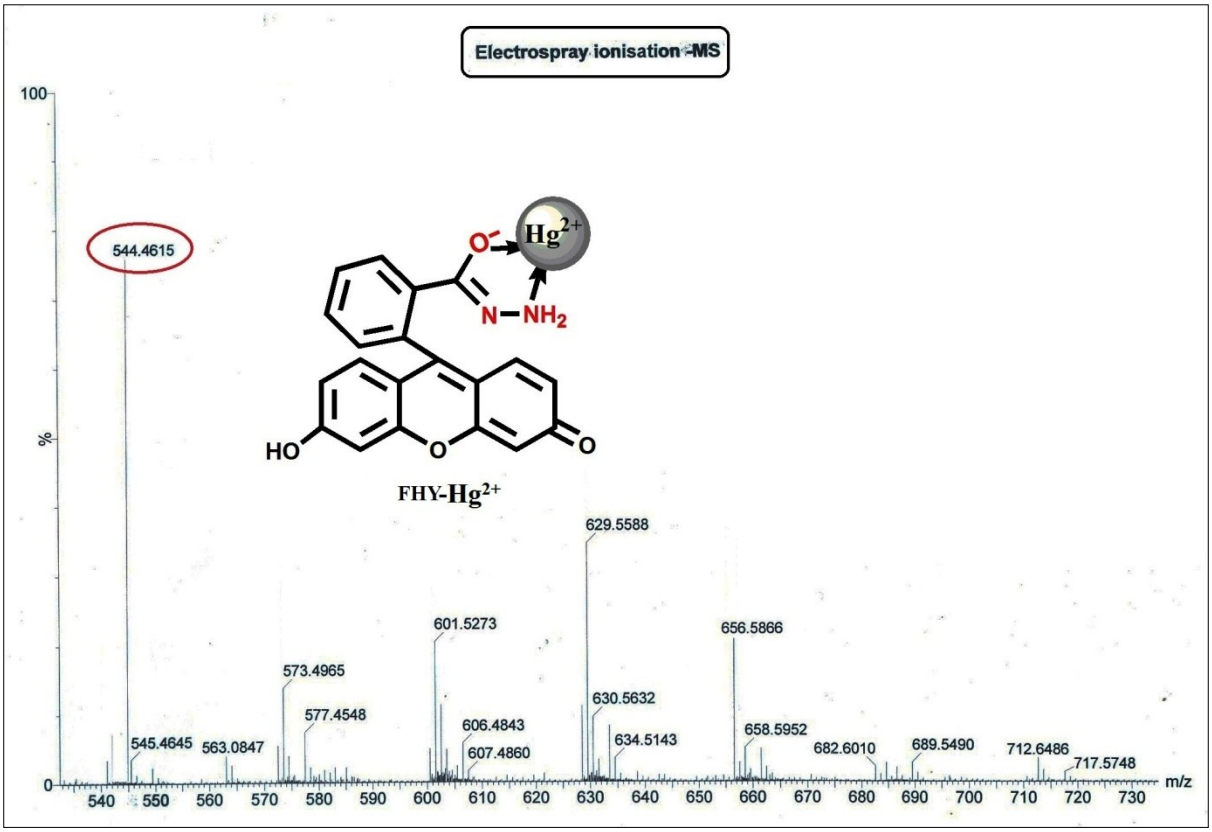

Figure S30. ESI- Mass spectrum of **FHY**–Hg^{2+}

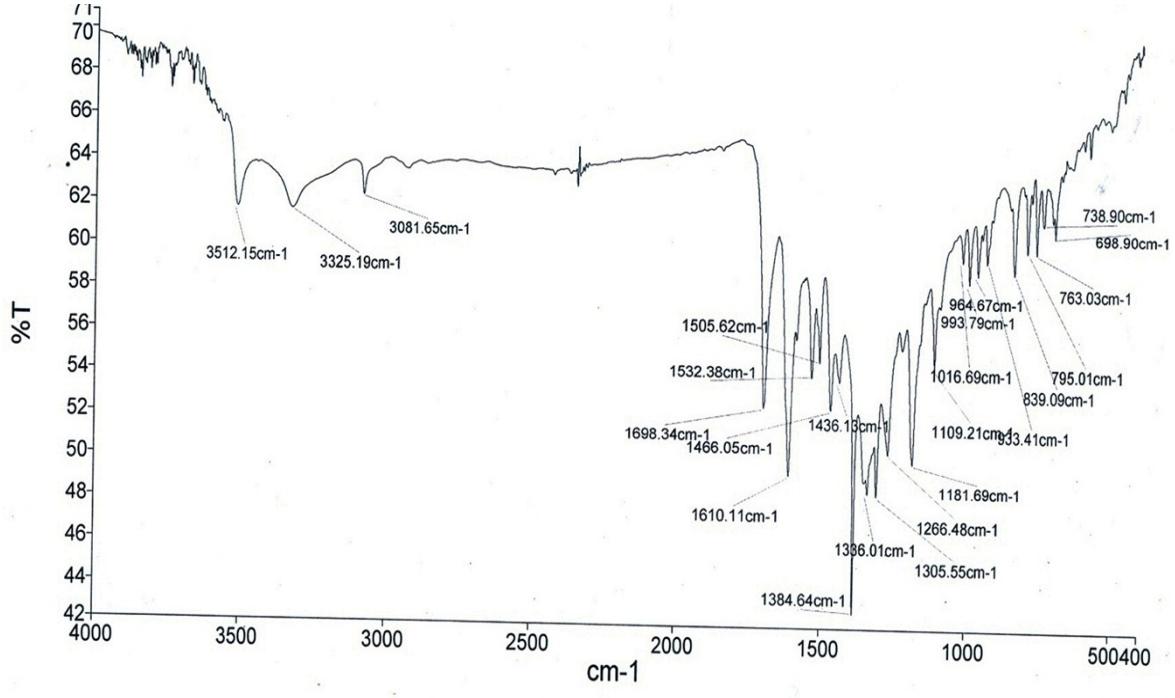

Figure S31. IR spectrum of **FHY**–Hg^{2+}

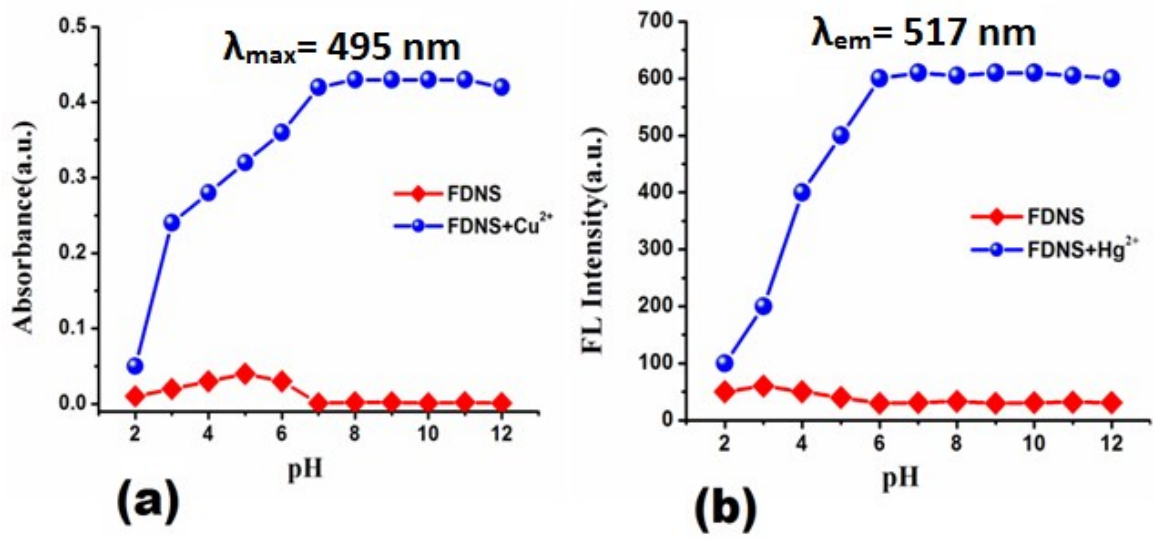

Figure S32. pH effects, **FDNS** in the presence of Cu^{2+} **(a)** and **(b)** Hg^{2+}

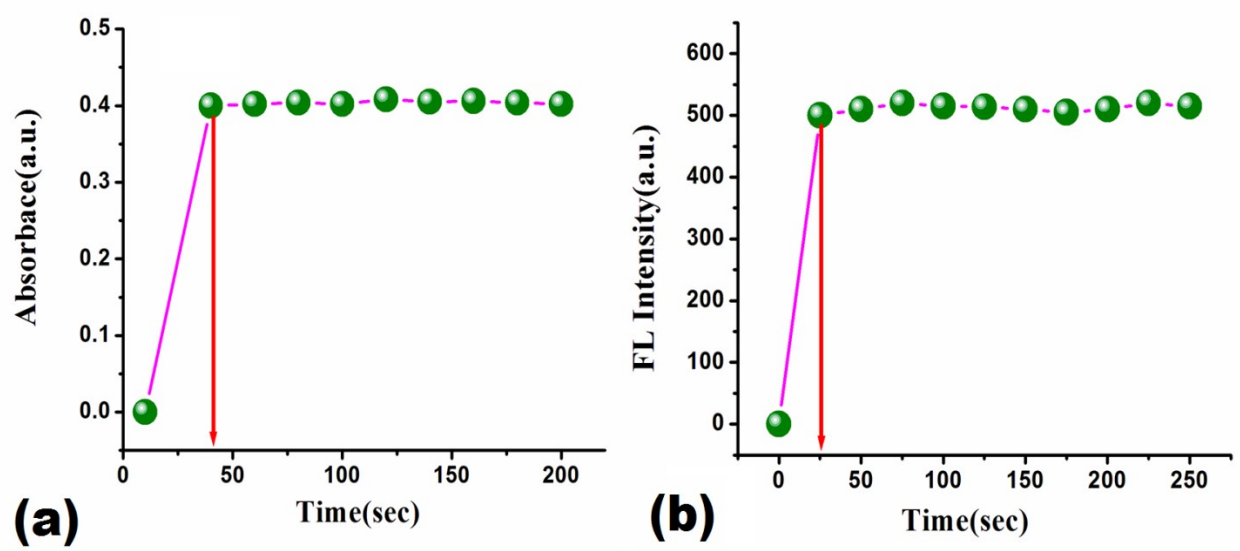

Figure S33. Reaction-time profile**: (a)** Changes of absorbance of **FDNS** in the presence of Cu^{2+} as a function of time (0-200 second) and **(b)** Changes of fluorescence of **FDNS** in the presence of Hg^{2+}as a function of time (0-250 second)

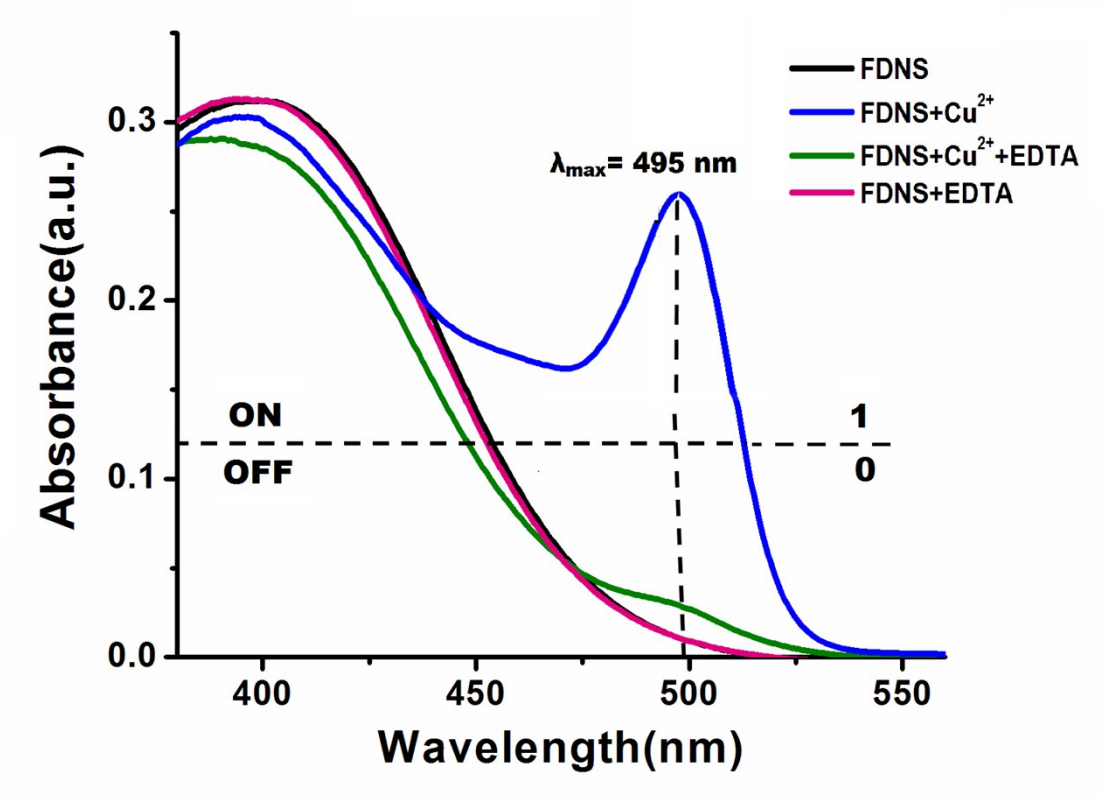

Figure S34. Absorption spectra of **FDNS** show changes at λmax = 495 nm with different input sequences and the assumed threshold value has been clearly marked here for construction of logic gate.

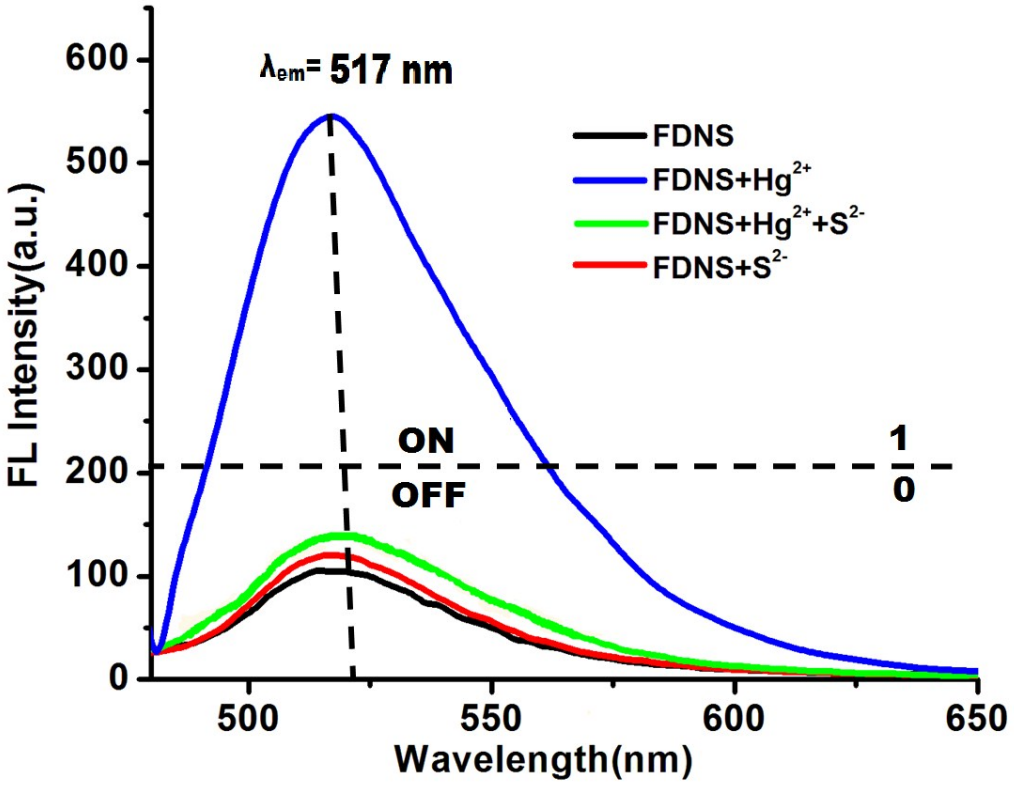

Figure S35. Emission spectra of **FDNS** show changes at λem = 517 nm with different input sequences and the assumed threshold value has been clearly marked here for construction of logic gate.

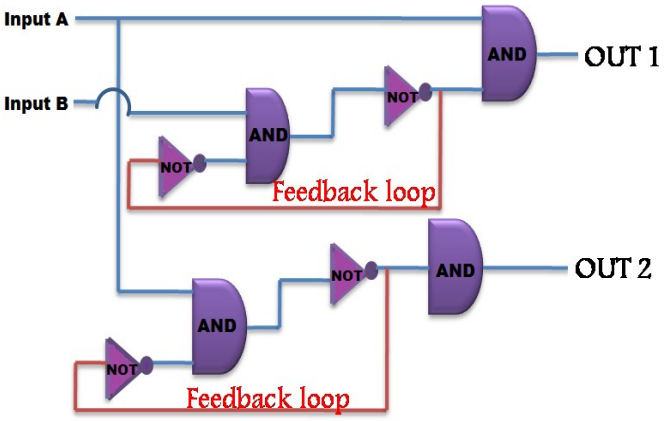

Input A Hg^{2+}	Input B S^{2-}	OUT1 λ_{em}= 517 nm	OUT2 Under UV light
0	0	0	0
0	1	0	0
1	0	1	1
1	1	0	0

Figure S36. Truth table and sequential logic circuits displaying memory units with two inputs (Input A (Hg^{2+}) and Input B (S^{2-}) and two outputs in the presence of chemical inputs.

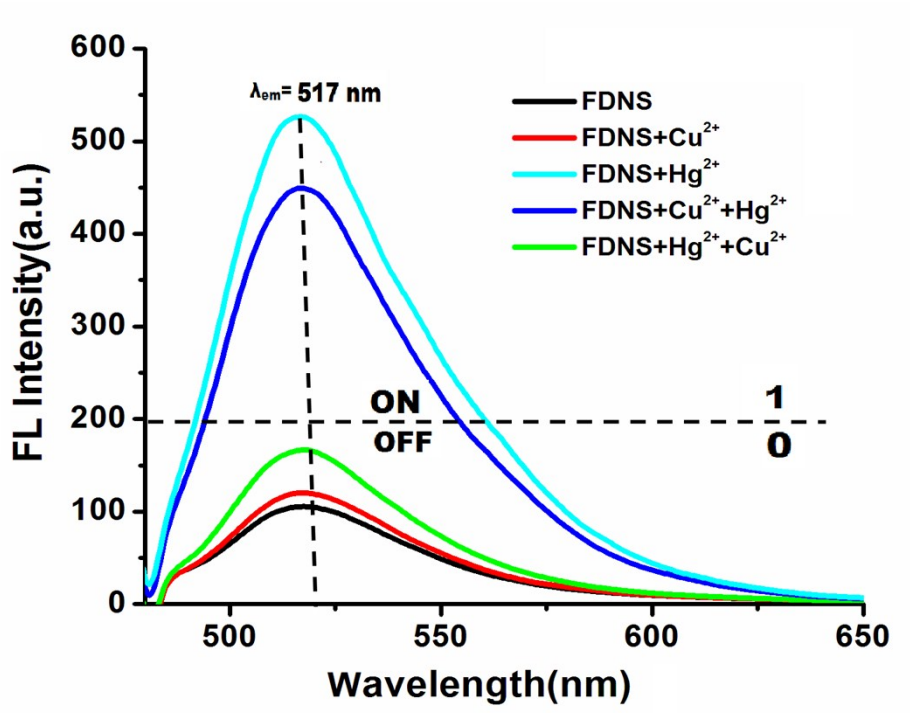

Figure S37. Emission spectra of **FDNS** show changes at λem = 517 nm with different input sequences and the assumed threshold value has been clearly marked here for designing molecular switch.

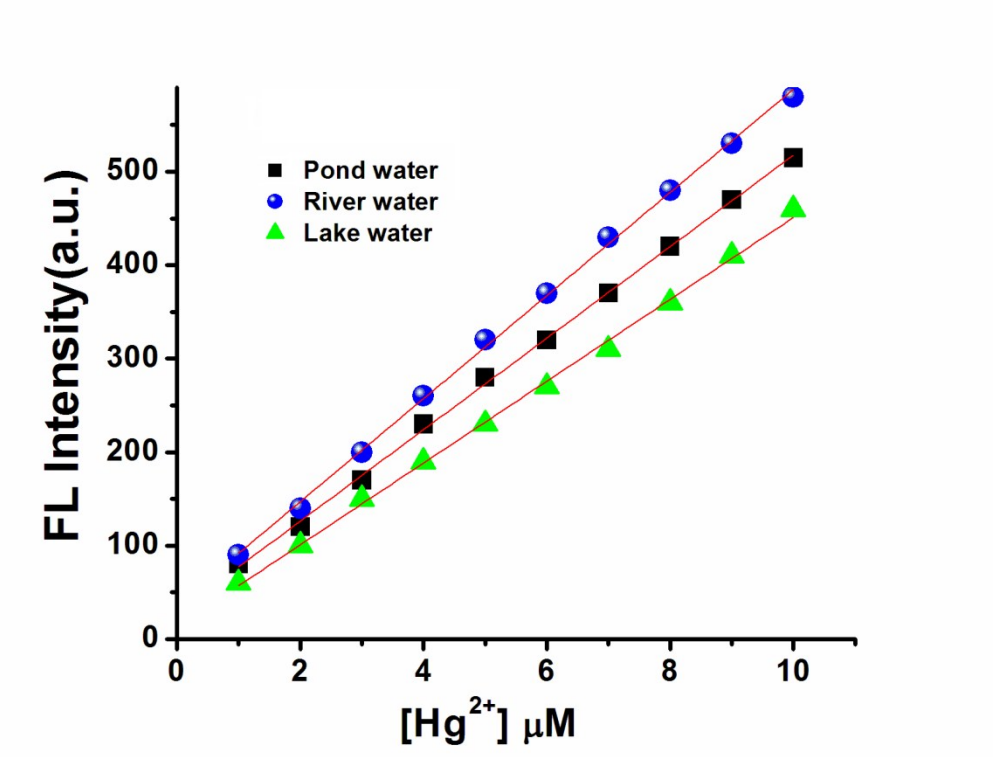

Figure S38. Proof-of-concept experiments with **FDNS** for determining Hg^{2+} (R^2 =0.99) in real water solutions.

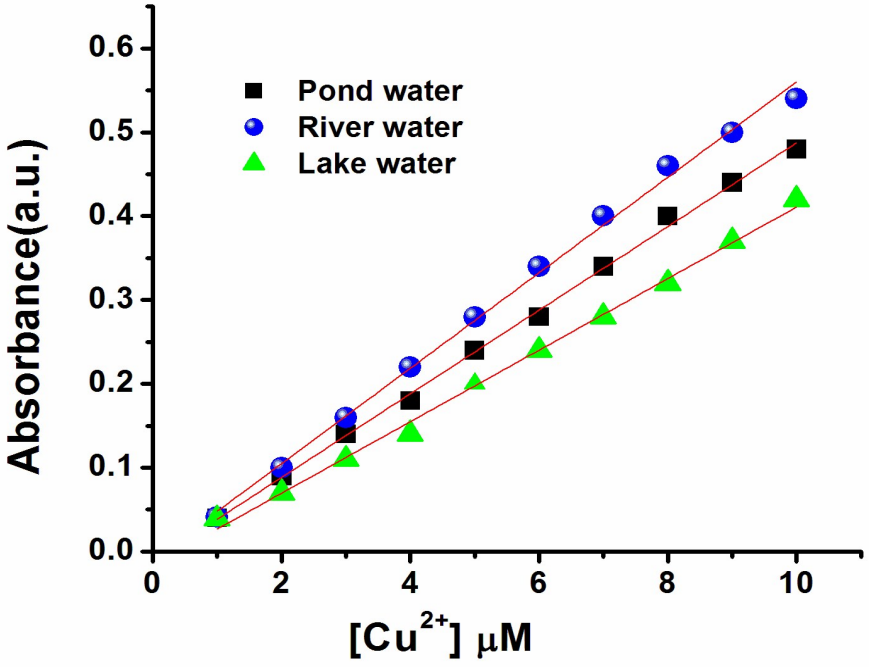

Figure S39. Proof-of-concept experiments with **FDNS** for determining Cu^{2+} ($R^2 = 0.99$) in real water solutions.

Table S1. Selected Crystallographic Data of **FDNS** and **FKCN.**

Parameters.	**FDNS**	**FKCN**
Formula.	$C_{27}H_{16}N_4O_{10}$	$C_{43}H_{53}N_5O_{10}$
M.	556.44	799.90
Crystal system.	Triclinic	Triclinic
Temperature(°K)	293(2)	293(2)
Space group.	*P*-1	*P*-1
a/Å	10.7051(13)	8.2826(5)
b/Å	11.1360(8)	13.7434(7)
c/Å	11.3232(11)	19.0467(9)
α(°)	78.976(7)	84.161(4)
β(°)	89.129(9)	86.179(4)
γ(°)	65.294(9)	77.400(4)
V/Å^3	1200.5(2)	2102.71(19)
Z	2	2
D_c/mg.m^{-3}	1.539	1.263
Reflns.collected/Unique	9846 / 5432	28490 / 10085
Data/restraints/Parameters.	5432 / 0 / 371	10085 / 1 / 531
R(int)	0.0561	0.0324
Limiting indices	-13<=h<=14 -12<=k<=14 -12<=l<=14	-11<=h<=11 -17<=k<=18 -25<=l<=26
θ range for data collection(°)	2.89- 28.98	3.05-29.35
Completeness to θ=25.00	99.8	99.8
Refinement method: Full-matrix, least-squares on F^2		
Final R indices[I>2σ(I)]	R_1= 0.0798 wR_2=0.1833	R_1=0.0813, wR_2=0.1842
R indices(all data)	R_1=0.1596, wR_2=0.2472	R_1=0.1219, wR_2=0.2087
GoF	1.002	1.042
Largest diff. peak and hole (e Å^{-3})	0.698 and -0.758	0.557 and -0.476

Table S2. Selected Bond Lengths (Å) and Bond Angles (deg) of **FDNS** and **FKCN.**

Bond angle	Deg (°)	Bond lengths(Å)	
FDNS			
N(10)-C(038)-C(022)	118.3(4)	N(8)-C(014)	1.507(5)
O(6)-C(030)-N(8)	124.4(3)	N(10)-N(8)	1.360(4)
C(038)-N(10)-N(8)	122.8(3)	N(8)-C(030)	1.383(4)
N(10)-N(8)-C(030)	116.6(3)	O(6)-C(030)	1.227(4)
N(10)-N(8)-C(014)	127.4(3)	O(5)-H(006)	0.8200
N(8)-C(014)-C(036)	113.0(3)	O(8)-C(018)	1.385(4)
O(4)-N(7)-O(3)	123.5(3)	O(8)-C(021)	1.394(4)
O(1)-N(3)-O(2)	121.5(4)	O(5)-C(16C)	1.331(4)
FKCN			
N(1)-C(008)-C(017)	121.5(2)	N(2)-C(015)	1.386(3)
O(4)-C(015)-N(2)	125.6(2)	N(1)-N(2)	1.373(3)
C(008)-N(1)-N(2)	117.8(2)	N(2)-C(006)	1.503(3)
N(1)-N(2)-C(015)	118.80(19)	C(015)-O(4)	1.212(3)
N(1)-N(2)-C(006)	126.93(18)	O(10)-H(10)	0.8200
N(2)-C(006)-C(005)	111.31(19)	O(2)-C(013)	1.386(3)
O(5)-N(5)-O(6)	120.2(3)	O(2)-C(014)	1.386(3)
O(7)-N(4)-O(8)	122.8(3)	O(3)-C(016)	1.259(3)
C(058)-N(3)-C(056)	110.9(3)	N(3)-C(058)	1.519(4)

Table S3. Selected parameters for weak interactions in **FDNS** and **FKCN**

D-H···A	D-H(Å)	H···A(Å)	D···A(Å)	D-H...A(°)	Symmetry code
FDNS					
O7--H003...O6	0.82	1.96	2.7765	172	1-x, 1-y, 1-z
O5--H006...N10	0.82	1.81	2.5452	148	
O9--H007....O1	0.82	2.40	2.9605	126	x, y, -1+z
O9--H007...O5	0.82	2.23	2.8964	139	x, y, -1+z
C023--H023....O6	0.93	2.59	3.2798	131	1-x, 1-y, 1-z
C032--H032...O4	0.93	2.56	3.4204	154	-1+x,1+y,z
FKCN					
O11 --H1W...O3	0.70	2.10	2.7381	151	1-x, -y, 1-z
O10 --H10....O11	0.82	1.86	2.6683	166	1+x, y, z
O1--H010....O3	0.82	1.98	2.7955	173	-1+x, y, z
C008--H1. ..O3	0.93	2.35	2.7346	105	
C056--H05A. ..O4	0.97	2.45	3.3891	162	
C056--H05B....O6	0.97	2.43	3.3818	168	-1+x, 1+y, z

Table S4. Data for analysis of Hg^{2+} ion in real sample by **FDNS**.

S.N.	Samples	Hg(II) added (μM)	Hg(II) found (μM)	% Recovery
1.	River Water	0	0	-
		2	1.92	96%
		4	3.86	96.5%
		6	5.74	95.66%
2.	Lake water	0	0	-
		2	1.89	94.5%
		4	3.85	96.25%
		6	5.79	96.5%
3.	Pond water	0	0	-
		2	1.89	94.5%
		4	3.86	96%
		6	5.77	96.16%

Table S5. Data for analysis of Cu^{2+} ion in real sample by **FDNS**.

S.N.	Samples	Cu(II) added (μM)	Cu(II) found (μM)	% Recovery
1.	River Water	0	0	-
		2	1.82	91%
		4	3.71	92.75%
		6	5.54	92.33%
2.	Lake water	0	0	-
		2	1.89	95.5%
		4	3.78	94.5%
		6	5.69	94.83%
3.	Pond water	0	0	-
		2	1.92	96%
		4	3.89	97.25%
		6	5.86	97.66%